INFORMATICS JOURNALS

Bio-Sourced Hydroxyapatite is Better Bioactive than its Synthetic Grade: A Comparative Assessment of Ti and Zn Doped Hydroxyapatite Derived from Bio and Synthetic Sources

Dalia Acharjee[1], Sujan Krishna Samanta[2], Sourav Debnath[3]*, Sukumar Roy[2], Piyali Basak[1] and Samit Kumar Nandi[4]

[1]*School of Bio-Science and Engineering Jadavpur University, Kolkata - 700032, West Bengal, India*

[2]*Department of Biomedical Engineering, Netaji Subhash Engineering College, Technocity, Garia, Kolkata - 700152, West Bengal, India*

[3]*Department of Electrical and Electronics Engineering, Swami Vivekananda Institute of Science and Technology, Kolkata - 700145, West Bengal, India; dr.souravdebnath@gmail.com*

[4]*Department of Veterinary Surgery and Radiology, WBUAFS, Kolkata - 700037, West Bengal, India*

Abstract

To meet everyday food requirements with an ever-increasing population in the world, a huge amount of Eggshell waste is given rise everywhere from household kitchens to various food processing units. Eggshell contains a large amount of calcium compound. In this study, two different kinds of Hydroxyapatite (HAp), one from different laboratory reagents and the other one from eggshell have been synthesized. 3% Titanium and Zinc doped variants have also been made for both kinds of Hydroxyapatite. The prepared powder samples were calcined at 800°C and pellets were formed by applying pressure. A comparative analysis of these two different sourced products has been made by analyzing physical properties (Density, apparent porosity, hardness), a functional group study (FTIR). The elemental configuration of all materials was confirmed by the EDAX study. XRD analysis revealed the lattice parameters of the pure product has been suffered a little bit with the doping agents. SEM images showed a significant amount of porosity and nodular grains of HAp. Cytotoxic analysis and MTT assay established the non-toxic nature of all compounds, In vitro SBF study showed apatite layer formation above the pellet surfaces of different grades and Ti-doped samples gained the maximum amount of apatite.

Keywords: *Eggshell Waste, SBF, SEM, XRD*

1.0 Introduction

To overcome the problems faced in autografting and allografting in bone tissue replacement surgeries[1] researchers pay heed to invent synthetically prepared bioceramics in the laboratory. Hydroxyapatite is one of the widely used bioceramics due to its osteoconductivity, biocompatibility, and close mechanical stability to human bone[2]. Several synthesis routes like wet chemical precipitation method[3-5], sol-gel preparation[6], Hydrothermal technique[7], multiple emulsion[8], biomimetic deposition[9,10], and electrodeposition technique[11] have been applied to prepare HAp by using various synthetic reagents in the laboratory. Several researchers used calcium

hydroxide as a source of calcium ions for preparing HAp in the laboratory[12], calcium nitrate as a starting reagent[13] can also be taken. Different processing parameters play an important role in the final properties of the synthesized powder[14]. Though the stoichiometric ratio of Ca/P (1.67) is maintained in synthetically prepared varieties it does not mimic the original bone composition stoichiometry due to the absence of different ions Fe^{+2}, Mg^{+2}, Si^{+2}, $Na^{+15,16}$. Researchers then searched and found to sort out the problem by using different biogenic sources as a source of calcium ions like animal bones (bovine, camel, horse), marine sources (fishbone, fish scale), shell sources (cockle, clam, Egg)[17-19]. Eggshell plays a vital role in getting hydroxyapatite as it contains about 94% of calcium carbonate[20]. Conversion of the eggshell to hydroxyapatite can minimize the eggshell waste causing environmental pollution. Although hydroxyapatite plays a potential role in bone graft surgeries, it has some limitations[21]. To enhance the mechanical strength and bioactivity[22,23], some trace elements as dopants can be added[24] to it. In this study, a comparative assessment has been made on synthetically derived and biogenic sourced hydroxyapatite along with their 3% Titanium and 3% Zinc doped variants.

2.0 Materials and Methods

2.1 Synthesis of Synthetic HAp, Eggshell HAp, and their Doped Variants

After collecting the discarded egg shells from different sources (home kitchen, University canteens, Street shops), it was boiled at about 60^0C temperature and washed several times with water to get rid of debris. The completely cleaned shells were triturated with mortar and pestle and calcined in the furnace at about 950^0C temperature with a heating rate of $5^0C/min$. Then a specified quantity of calcined powdered eggshell was added slowly in warm water, and a stoichiometric amount of orthophosphoric acid (0.6M) was added to the mixture with vigorous stirring by a magnetic stirrer while maintaining the 11-12. The mixture was kept in cool and dark places for precipitation. The precipitate was separated and dried in a hot air oven at about 800^0C temperature. The dried samples were calcined in the furnace at 800^0C temperature. For synthetic HAp (mentioned as pure HAp in this literature), laboratory-grade calcium hydroxide powder was reacted

with orthophosphoric acid. To prepare the doped variants, a stoichiometric quantity of titanium oxide and Zinc oxide powder was added to the mother powder [Eggshell/$Ca(OH)_2$ powder] before adding acid to the solution.

2.2 Pellet Formation and Physical Properties Measurement

The accumulated lump calcined samples were ball milled for about 2 hours to get fine grains of powder. The sample powders were pressed hard (2 tons for 2 minutes) through a hydraulic press machine (PEECO Pvt Ltd, India) with a cylindrical mold having an internal diameter of 12 mm. The formed pellets had a 5 ± 0.05 mm thickness. The density of the pellets (green density) was measured. The pellets were sintered at about 900^0C temperature and again the density was calculated. In this study, hardness was measured by Vickers hardness tester machine (VM 50, Instr. and Engg. India).

2.3 XRD, FTIR Analysis

Phase analysis, lattice parameters, percentage crystallinity, and unit cell volume were calculated by using an X-ray diffractometer (Bruker 8, Japan) in a range of 200-600. The lattice parameter was measured by using the Unit cell plane spacing relationship of HCP[25].

$$\frac{1}{d^2} = \frac{4}{3}\left(\frac{h^2+hk+k^2}{a^2}\right) + \frac{l^2}{c^2}$$

where d is the distance between the next adjacent planes in the conventional set of Miller indices (h k l). The unit cell volume (V) was calculated using the relation $V = 0.866\ a2c$[26]. The crystallite size of the powder samples was calculated by Scherrer's equation,

$D = 0.9\ \lambda/\beta cos\theta$[26]. Where D is the size of the crystal, λ is the X-ray wavelength, β is the diffraction line broadening at half of its maximum intensity in radians and θ is the diffraction angle. The presence of the functional group was confirmed through FTIR analysis (Perkin-Elmer-1615, US) in the wavelength range of 500-4000 cm^{-1}.

2.4 SEM and EDAX Study

The microstructure and surface morphology were examined using Scanning Electron Microscopy (SEM).

The grain size, presence of pores and its size, and nature of crystal formation were also investigated. The sintered pellets of HAp and its dopants were crushed by a hammer. The surfaces were studied under a Scanning Electron Microscope (JEOL SEM, Model No-JSM, 5200, TOKYO, Japan). For analysis, three different SEM images from each sample were captured and for reporting, the average value was calculated.

The microstructure of the dense samples was assessed for the influence of the dopant ion incorporation during the high-temperature processing. The EDAX study signifies the presence of different elements in the samples.

2.5 Bioresorption Study

The dissolution property/behavior of HAp and its doped ceramic in a physiological environment was carried out through an in-vitro dissolution study by immersing the samples in Simulated Body Fluid (SBF) solutions. In this Bioresorption study, the fluid was prepared by the Kokubo method[27]. The solution was placed in an incubator by maintaining a pH of 7.25 and was changed every three alternate days. The study experiment was continued for one month. The apatite layer formation above the pellet surfaces was studied through Scanning electron microscopy.

2.6 Bactericidal Study

A bactericidal study was done to ensure whether the compositions have any kind of antimicrobial properties or not. In this present study diluted solution of nutrient agar media was taken in a conical flask and autoclaved at 121^0C temperature for 20 mins. The media was then cooled to 40-45 ^0C temperature and inoculated with the culture of *Staphylococcus aureus*. After a thorough mixing of the culture with media, these contents were then poured into Petri dishes and they became solidified. The porcelain bit was dripped into the sample powder solution and placed in the Petri dishes. Two different bits having different strengths (3mg/10ml and 1mg/10ml) were taken. The Petri dishes were incubated at 35^0C temperature for 24 hours.

2.7 MTT Assay

Peripheral Blood Mononuclear Cells (PBMC) cells (NCCS, Pune) were used for the MTT assay. After seeding the cells in 24 well plates (Density-5 x 10^4 cells/ cm^2), samples were added and incubated for 24 hours. Then, MTT was added with in-depth shaking for about 15 min and again incubated for four hours. The formed crystals were dissolved in Dimethyl sulfoxide solvent and appeared with a purple-colored solution. The optical density of the solution was taken at 545nm range against a blank. The experiment was repeated three times and the final result was taken by making an average.

2.8 Hemolysis Study

The methodology for this study was followed as described in the ASTM specification[28]. Anticoagulant (3.8% Sodium Citrate solution) added human blood (10:1) and Normal Saline (NS) solution in 4:5 ratio was used to prepare a diluted blood sample. Pellets of each sample were taken in a test tube containing 10 ml NS and incubated at 370C for 30 min. Then, 0.2 ml of diluted blood was added to each test tube and further incubated at 370C for 1 hour. For the preparation of the positive control solution, 0.2 ml diluted blood was added in a test tube containing 10 ml Na_2CO_3 (0.1%) solution, and for the negative control solution, 0.2 ml diluted blood was added in another test tube containing 10 ml of normal saline solution. Both the positive and negative control solutions were incubated at 370C temperature for 1 hour. After incubating, all these test tubes were centrifuged at a speed of 500g for 5 min. The supernatant liquid was taken measuring the optical density at 545 nm wavelength in a UV-V is spectrophotometer (Elico India, SL- 177).

3.0 Results and Discussion

3.1 Physical Properties

The experimented data of different studies are tabulated in Table 1.

The hardness for all the different specimens is mostly the same in order and revealed a significant value, which can be able to sustain the imported load that may come to the healing area. The green density of the samples has drastically changed with the application of heat, and the sintered density data are quite higher and almost double than green density for all samples. Both the Zinc and Titanium doped eggshell HAp showed the maximum percentage of porosity compared to other samples. Pure

Table 1. Different physical properties

Specimen	Hardness (Gpa)	Avg. Green Density (g/c.c.)	Avg. Sintered Density (g/c.c.)	Apparent porosity (%)	Pore size distribution (µm)
Pure HAp	3.64 ± 0.030	1.53 ± 0.022	2.97 ± 0.015	22.02 ± 1.66	10-112
Egg shell HAp	3.71 ± 0.020	1.546 ± 0.011	2.94 ± 0.0115	30.48 ± 1.72	8-100
Pure HAp+Zn3%	3.78 ± 0.031	1.6 ± 0.015	3.06 ± 0.021	25.91 ± 1.94	14-123
Eggshell HAp+Zn3%	3.92 ± 0.031	1.602 ± 0.008	3.03 ± 0.0153	37.13 ± 0.96	12-105
Pure HAp+Ti3%	3.83 ± 0.015	1.564 ± 0.016	3.02 ± 0.016	24.31 ± 2.48	11-112
Egg shell HAp+Ti3%	3.98 ± 0.036	1.562 ± 0.020	2.97 ± 0.0378	34.90 ± 1.06	7-110

Table 2. Lattice parameters data

Parameters	Pure HAp	Eggshell HAp	Pure HAp+Zn$_3$%	Eggshell HAp+Zn$_3$%	Pure HAp+Ti$_3$%	Eggshell HAp+Ti$_3$%
a-axis (Å)	9.423 0 ± .0.09 7	9.416 ± 0.11	9.3130 ± .0.097	9.321 ± 0.51	9.373 ± .0.097	9.351 ± 0.51
c axis (Å)	6.841 ± 0.120	6.787 ± 0.17	6.641 ± 0.120	6.627 ± 0.17	6.681 ± 0.120	6.687 ± 0.17
Unit cell volume (Å3)	533.9 3 ± 22.02	521.05 ± 18.29	515.78 ± 22.54	497.05 ± 18.29	508.91 ± 16.29	498.97 ± 19.16
Crystallite size (Å)	3.628 6 ± 12.67	3.5556 ± 9.84	3.3381 ± 11.57	3.2921 ± 14.77	3.3621 ± 8.02	3.3212 ± 11.12
%Crystallinity	93.81 ± 3.82	84.81 ± 5.76	84.41 ± 4.12	86.01 ± 5.76	84.47 ± 6.82	89.46 ± 4.02

HAp-derived doped samples contain less percent of porosity (below 26% in both cases of Zn and Ti doped samples). The percentage of porosity is higher on eggshell samples may be due to its biogenic nature and owe to huge amount of carbonate contents. The Titanium and Zinc doped derivatives of both HAp (pure and Eggshell) showed more percentage porosity than their own pure form. It may be attributed to the substituted lattice leaving more spaces in the unit cell structure.

3.2 XRD Study

XRD spectra of different samples show various prominent peaks, corresponding to different planes i.e., (0 0 2), (2 11), (2 0 2), (3 0 0), (2 1 2), (2 2 2). These are very much corresponding to standard reference card no 09-0432 meant for crystallite hydroxyapatite structure. The intensity value of the peaks of all the samples in corresponding planes are more or less the same, but in
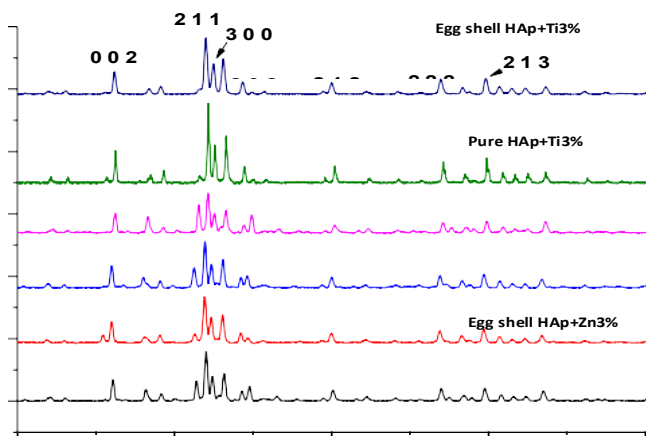
Figure 1. XRD of Pure HAp, Eggshell HAp, and dopants.

Titanium and zinc-doped variants the peaks are slightly shifted.

The study showed that the lattice parameters suffered minor changes perceptibly from the incorporation of different dopants. The values of both the a and c axes decreased systematically in all the cases and are shown in below Table 2. This may be caused by the smaller atomic radii of the dopants e.g., Zinc (134 pm), and Titanium (147 pm) as compared to Ca (197 pm). The results confirmed the substitution of calcium ions by the dopants and the consequent reduction in unit cell dimensions.

3.3 FTIR Analysis

Figure 2 depicts the FTIR plot of all the samples. Almost the same kind of FTIR spectra have been revealed. Sharp

Figure 2. FTIR of Pure HAp, Eggshell HAp, and their dopants.

peaks at 562 and 1031 indicate the presence of phosphate ions whereas at 3722, a stretching band of hydroxyl ions is present.

3.4 SEM and EDX Study

The SEM images of all the different types of samples are shown in Figure 3. It supports the sufficient number of nodular-shaped pores present in the sample which are essential for bony ingrowth throughout it. The presence of pores gives the structural integrity of the scaffolds.
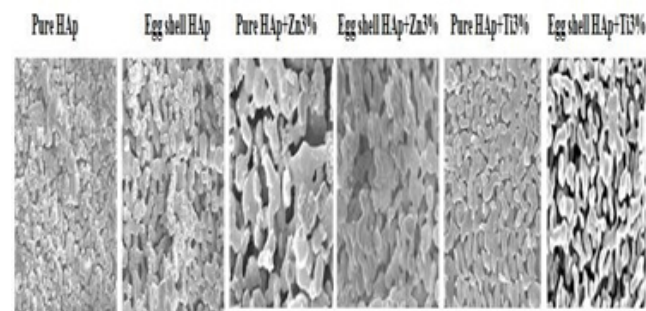

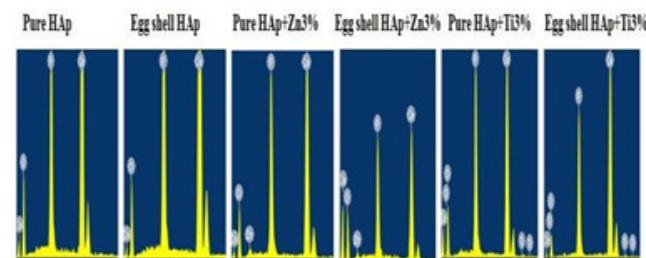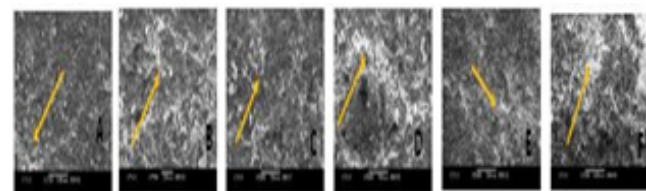**Figure 3.** SEM images of Pure HAp, Eggshell HAp, and their dopants.

Figure 4. E-DAX of Pure HAp, Eggshell HAp, and their dopants.

Figure 5. Apatite images of Pure HAp, Eggshell HAp, and their dopants, Yellow arrows are showing the apatite formation area.

Elemental analysis through the E- DAX study provides the presence of calcium, phosphorus, and trace elements of zinc, and titanium ions.

3.5 SBF Study

Apatite layer formation above the sintered pellets after 7 days was noticed through the scanning electron microscopy method. The size and thickness of the apatite layer were increased by increasing the immersion times.

3.6 Bactericidal and MTT Assay Study

In the bactericidal study, all the Petri dishes showed (Figure 6) no zone of inhibition after 24 hours of incubation. This suggests, that the concentration (1mg/10
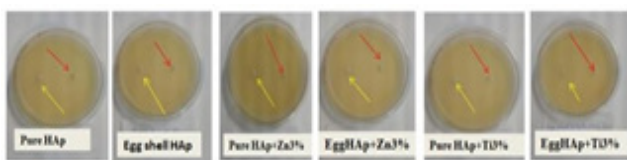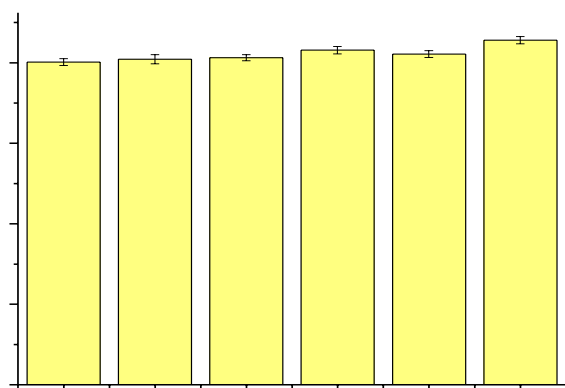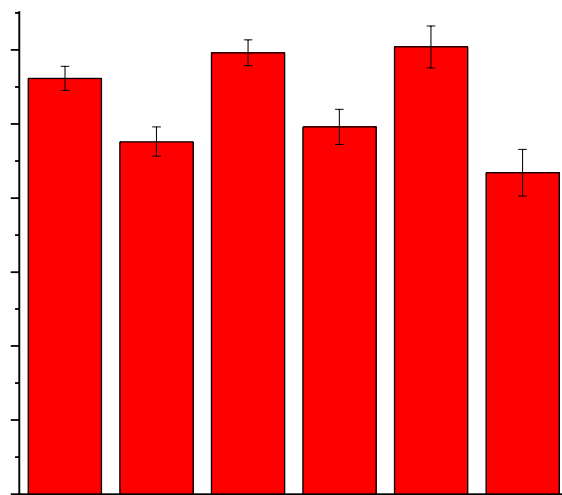

Figure 6. Petri dishes showing culture media of Pure HAp, Eggshell HAp, and their dopants (Red arrow and yellow arrow show the sample concentration in porcelain bit of 3mg/10ml and 1mg/10ml respectively).

S6-Egg shell HAp+Ti3%
S5-Pure HAp+Ti3%
S4-Egg shell HAp+Zn3%
S3-Pure HAp+Zn3%
S2-Egg shell HAp
S1-Pure HAp

Figure 8. Bar diagram showing percent cell viability of samples.

S6-Egg shell HAp+Ti3%
S5-Pure HAp+Ti3%
S4-Egg shell HAp+Zn3%
S3-Pure HAp+Zn3%
S2-Egg shell HAp
S1-Pure HAp

Figure 8. Bar diagram showing the percent of hemolysis.

ml and 3mg/10 ml) of Pure HAp and Eggshell HAp and its dopants possess no bactericidal properties. Although zinc ions showed some antibacterial activities, this is a very small amount and can be considered as no zone of inhibition. The eggshell HAp and their dopant (3%Zn and 3%Ti) variant show similar kind of properties as pure HAp.

The bar diagram representing the percentage of cell viability in Figure 7 depicted that all the six category samples exhibited more than eighty percent cell viability after one day of incubation. Eggshell HAp and their 3% Zn and 3% Ti doped variants showed a little bit more percentage viable cells than pure HAp and their doped variants.

The percentage of hemocompatibility is less than 5% for all samples. So according to the ASTM guidelines, all samples are highly hemocompatible. Among the different compositions S6 sample i.e., 3% titanium-doped eggshell Hap shows the maximum percentage of hemocompatibility.

4.0 Conclusion

The hydroxyapatite has been synthesized successfully from eggshell waste, a biogenic source. The phase

analysis, and lattice parameter study showed its nodular crystal configuration. The FTIR and E-DAX studies expressed the presence of desired functional groups and elements. The porous nature of the scaffold samples was evidenced through SEM pictures and apparent porosity values. MTT assay and hemolysis study revealed that all the compositions were nontoxic and hemocompatible in nature. A comparative analysis of SEM images of SBF-treated pellets confirmed that the distribution and density of the apatite layer are more in biogenic sourced hydroxyapatite than synthetic source (Pure HAp) derived samples. Hence it can be concluded that biosourced-derived hydroxy apatite is more bioactive and can be used as a potential bone graft material.

5.0 References

1. Nandi SK, Kundu B, Ghosh SK, De DK, Basu D. Efficacy of nano-hydroxyapatite prepared by an aqueous solution combustion technique in healing bone defects of goat. J Vet Sci. 2008; 9(2):183–91. https://doi.org/10.4142/jvs.2008.9.2.183

2. Hench LL, Wheeler DL. J Sol-Gel Sci Technol. 1998; 13:245–50. https://doi.org/10.1023/A:1008643303888

3. Santos MH, de Oliveira M, de Freitas Souza P, Mansur HS, Vasconcelos WL. Synthesis control and characterization of hydroxyapatite prepared by wet precipitation process. Mater Res. 2004; 7(4):625- 630. https://doi.org/10.1590/S1516-14392004000400017

4. Manuel CM, Ferraz MP, Monteiro FJ. Nanoapatite and microporous structures of hydroxyapatite. Proceeding of the 17th European Society of Biomaterials. Barcelona, Spain. 2002; T 153.

5. Manuel CM, Ferraz MP, Monteiro FJ. Synthesis of hydroxyapatite and tricalcium phosphate nanoparticles. Preliminary Studies. Key Eng Mater. 2003; 240-242:555-58. https://doi.org/10.4028/www.scientific.net/KEM.240-242.555

6. Chai CS, Ben-Nissan B. Bioactive nanocrystalline sol-gel hydroxyapatite coatings. J Mater Sci MaterMed. 1999; 10:465-9. https://doi.org/10.1023/A:1008992807888

7. Manafi SA, Joughehdoust S. Synthesis of hydroxyapatite nanostructure by hydrothermal condition for biomedical application. Iranian JPharm Sci. 2009; 5(2):89-94.

8. Kimura I. Synthesis of hydroxyapatite by interfacial reaction in a multiple emulsion. Res Lett Mater Sci. 2007; 71284:1-4. https://doi.org/10.1155/2007/71284

9. Tas AC. Synthesis of biomimetic Cahydroxyapatite powders at 37 degrees C in synthetic body fluids. Biomaterials. 2000; 21:1429-38. https://doi.org/10.1016/S0142-9612(00)00019-3

10. Thamaraiselvi TV, Prabakaran K, Rajeswari SS. Synthesis of hydroxyapatite that mimics bone mineralogy. Trends Biomater Artif Org. 2006; 19(2):81-3.

11. Shikhanzadeh M. Direct formation of nanophase hydroxyapatite on cathodically polarized electrodes. JMater Sci: Mater Med. 1998; 9:67-72.

12. Ansari M, Naghib SM. Synthesis and characterization of hydroxyapatite calcium hydroxide for dental composites. Ceramics – Silikáty. 2011; 55(2):123-6.

13. Alobeedallah H, Ellis JL, Rohanizadeh R. Preparation of nanostructured hydroxyapatite in organic solvents for clinical applications. Trends Biomater Artif Organs. 2011; 25(1):12-9.

14. Salma K, Berzina-Cimdina L, Borodajenko N. Processing and application of ceramics. 2010; 4(1):45-51. https://doi.org/10.2298/PAC1001045S

15. Milovac D, et al. PCL-coated hydroxyapatite scaffold derived from cuttlefish bone: Morphology, mechanical properties and bioactivity. Mater Sci Eng. 2014; 34:437e445. https://doi.org/10.1016/j.msec.2013.09.036

16. Akram M, et al. Extracting hydroxyapatite and its precursors from natural resources. J Mater Sci. 2014; 49(4):1461e1475. https://doi.org/10.1007/s10853-013-7864-x

17. Herliansyah MK, Nasution DA, Hamdi M, Ide-Ektessabi A, Wildan MW, Tontowi AE. Preparation and characterization of natural hydroxyapatite: A comparative study of bovine bone hydroxyapatite and hydroxyapatite from calcite. Mater Sci Forum. 2007; 561–565:1441–4. https://doi.org/10.4028/www.scientific.net/MSF.561-565.1441

18. Panda NN, Pramanik K, Sukla LB. Extraction and characterization of biocompatible hydroxyapatite from freshwater fish scales for tissue engineering scaffold. Bioproc Biosyst Eng. 2014; 37:433–40. https://doi.org/10.1007/s00449-013-1009-0

19. Mustaffa R, Mohd Yusof MR, Abdullah Y. A novelty of synthetic hydroxyapatite from cockle shell and characterization. Adv Mater Res. 2015; 1087:429–33. https://doi.org/10.4028/www.scientific.net/AMR.1087.429

20. Akram M, Ahmed R, Shakir I, Ibrahim WAW, Hussain R. Extracting hydroxyapatite and its precursors from

natural resources. J Mater Sci. 2014; 49:1461–75. https://doi.org/10.1007/s10853-013-7864-x

21. Webster TJ, Massa-Schlueter EA, Smith JL, Slamovich EB. Biomaterials. 2004; 25:2111–21. https://doi.org/10.1016/j.biomaterials.2003.09.001

22. Mardziah CM, *et al*. Effect of zinc ions on the structural characteristics of hydroxyapatite bioceramics. Ceram Int. 2020; 46(9):13945–52. https://doi.org/10.1016/j.ceramint.2020.02.192

23. Uskoković V. Ion-doped hydroxyapatite: An impasse or the road to follow? Ceram Int. 2020; 46(8):11443–65. https://doi.org/10.1016/j.ceramint.2020.02.001

24. Liu X, Man HC. Laser fabrication of Ag-HA nanocomposites on Ti$_6$Al$_4$V implant for enhancing bioactivity and antibacterial capability. Mater Sci Eng. 2017; 70:1-8. https://doi.org/10.1016/j.msec.2016.08.059

25. Kim JH, Kim SH, Kim HK, Akaike T, Kim SC. Synthesis and characterization of hydroxyapatite crystals: A review study on the analytical methods. J Biomed Mater Res. 2002; 62(4):600–12. https://doi.org/10.1002/jbm.10280

26. Cullity BD. Elements of diffraction quasi-optics, second., no. 1. London-Amstrerdam-Don Mills, Ontario-Sydney: Addison-Wesley Publishing Company Inc; 1977.

27. Kokubo T, Kushitani H, Sakka S, Kitsugi T, Yamamuro T. Solutions able to reproduce *in vivo* surface- structure changes in bioactive glass-ceramic A-W3. J Biomed Mater Res. 1990; 24(6):721–34. https://doi.org/10.1002/jbm.820240607

28. ASTM F 756-00. Standard practice for assessment of hemolytic properties of materials. Philadelphia. Am Soc Test Mater. 2000; 5. https://doi.org/10.1520/F0756-13